J. Serb. Chem. Soc. 71 (12) 1333–1343 (2006) UDC 547.261+66.094.3+541.135.5+546.92:541.128
JSCS–3526 *Original scientific paper*

Methanol oxidation at platinum electrodes in acid solution: comparison between model and real catalysts

A. V. TRIPKOVIĆ[a*], S. LJ. GOJKOVIĆ[b#], K. DJ. POPOVIĆ[a#] and J. D. LOVIĆ[a#]

[a]*ICTM-Institute of Electrochemistry, University of Belgrade, Njegoševa 12, P. O. Box 473, 11000 Belgrade, Serba and* [b]*Faculty of Technology and Metallurgy, University of Belgrade, Karnegijeva 4, P. O. Box 3503, 11000 Belgrade (e-mail: amalija@tmf.bg.ac.yu)*

(Received 8 December 2005, Revised 15 March 2006)

Abstract: Methanol oxidation in acid solution was studied at platinum single crystals, Pt(*hkl*), as the model catalyst, and at nanostructural platinum supported on high surface area carbon, Pt/C, as the real catalyst. The linear extrapolation method was used to determine the beginning of hydroxyl anion adsorption. Structural sensitivity of the adsorption was proved and a correlation with the onset of the methanol oxidation current was established at all catalysts. Bisulfate and chloride anions were found to decrease the methanol oxidation rate, but probably did not influence the reaction parth. The specific activity for the reaction increased in the sequence Pt(110) <Pt/C < Pt(111), suggesting that the activity of the supported Pt catalyst can be correlated with the activities of the dominating crystal planes on its surface.

Keywords: methanol oxidation; Pt(*hkl*); Pt supported catalyst; acid solution.

INTRODUCTION

Methanol oxidation on platinum electrodes in an acid electrolyte is a catalytic reaction producing CO_2 and six electrons per one CH_3OH molecule:

$$CH_3OH + H_2O \rightarrow CO_2 + 6H^+ + 6e^- \quad (1)$$

Although the standard equilibrium potential of methanol oxidation is 0.02 V, a reasonable reaction rate can be achieved at potentials shifted several hundreds of milivolts in the positive direction due to the difficulty in the oxidation of adsorbed intermediates.[1]

Methanol oxidation on platinum is an important reaction since it has potential for fuel cell application (direct methanol fuel cell, DMFC).[2] It has been extensively studied using electrochemical methods as well as spectroscopic techniques.[3–10] Studies on single crystal Pt samples have shown that methanol oxidation

* Corresponding author.

Serbian Chemical Society active member.

doi: 10.2298/JSC0612333T

is a strongly structure sensitive reaction.[11,12] Dehydrogenation of methanol in successive steps[13] suggests the presence of several adsorbates. Spectroscopic techniques applied *in situ* on single crystal platinum have proved only CO_{ad}[14,15] and COH_{ad} or CHO_{ad} species.[16] Adsorbed CO was proposed to have a dual role, *i.e.,* it acts as a poison, especially at lower potentials, and also as a reactive intermediate.[1,5] Adsorbed OH generated from a H_2O molecule[17–19] or even some activated H_2O molecule adsorbed on the Pt surface[20] were assumed as the participants in the reaction necessary to oxidize CO_{ad}.

The fact that methanol is a good candidate for DMFC explanded the study of its oxidation on so-called real catalysts, such as Pt nanostructured catalysts formed by deposition of Pt particles on high area carbon.[21–24] In this work, a comparison between the results obtained in methanol oxidation on Pt(*hkl*) and on Pt nanostructured catalyst (Pt/C), in acid solution is presented.

EXPERIMENTAL

Electrode preparation

The platinum low-index single crystal electrodes were purchased from Metal Crystal and Oxides Ltd., (Cambridge, UK) and oriented to better than 1°. Standard mechanical polishing of the surface was followed by annealing in a hydrogen flame with cooling in a hydrogen stream. The almost cool crystal was protected by a water drop and transferred into an electrochemical cell.[25] Voltammetric curves in the hydrogen adsorption/desorption region were used to estimate the two-dimensional order of the surface.

The carbon supported Pt electrode, assigned as Pt–C/GC, was formed by deposition of a commercially available Pt/C catalyst with a loading of 47.5 wt % Pt (Tanaka Precious Metal Group) on a glassy carbon disk. The thin catalyst layer was prepared by attaching ultrasonically re-dispersed catalyst suspension in high-purity water onto the glassy carbon, resulting in a constant metal loading of 20 μg_{Pt} cm^{-2}.[26] After drying in flowing high purity argon at room temperature, the deposited catalyst layer was covered with 20 μl of a diluted aqueous Nafion solution (thickness of *ca*. 0.2 μm) and, finally, the electrode was immersed in nitrogen purged electrolyte.

Electrode characterization

As previously described,[27] low energy electron diffraction (LEED) measurements showed clean, well-ordered unreconstructed Pt(*hkl*) surfaces. The results of the characterization of the Pt/C catalyst can be briefly summarized as follows.[27,28] TEM Analysis showed a reasonably uniform distribution of Pt particles on the carbon support. Typical highly faceted cubooctahedral Pt nanoparticles were detected by HRTEM.[27] The histogram of the particle size distribution demonstrated that the particle size ranged between 2–6 nm, with an average diameter of 4±0.3 nm.[28] AFM and STM images showed that the particles of the Pt/C catalyst deposited on glassy carbon were in the form of 3D agglomerates of several tens of nm with Pt particles with a diameter mostly between 2 and 7 nm on the top of them.[27] Calculation based on XRD measurements revealed an average size of 3.1 nm.[29]

At the beginning of each experiment, the real surface area of the supported Pt electrode was estimated using a conventional procedure based on the coulometry of H_{upd} (taking 210 μC cm^{-2} for a monolayer). The specific surface area was calculated as $S_{sp} = S/m_{Pt}$, where S is the real surface area and m_{Pt} is the mass of Pt in the catalyst layer. The average diameter of the Pt particles was calculated assuming a spherical shape of the particles[30] by using the equation: $d = 6 / \rho S_{sp}$, where ρ is the density of platinum (ρ = 21.4 g cm^{-3}). The parameters of the Pt/C deposits on GC electrodes are given in Table I.

TABLE I. Parameters of the Pt/C catalyst deposited on a glassy carbon electrode (GC)

GC Geometric area, A_G/cm^2	0.283
Pt Loading/μg cm^{-2}	20.0
Pt Total mass, m_{Pt}/μg	5.66
Pt Real surface area, S/cm^2	3.62
Pt Specific area, S_{sp}/m^2 g^{-1}	64.2
Average Pt particle diameter, d/nm	4.3

The average Pt particle diameter determined by microscopic and spectroscopic techniques is in agreement with the value of 4.3 nm calculated on the basis of H_{UPD} coulometry given in Table I.

Electrochemical measurements

All electrochemical measurements were conducted in a thermostated three-compartment electrochemical cell with a Pt spiral as the counter electrode and a saturated calomel electrode as the reference electrode. All the potentials reported in this paper are expressed on the scale of the reversible hydrogen electrode (RHE). The electrolyt contained 0.1 M $HClO_4$ or 0.1 M H_2SO_4 as supporting electrolyte and 0.5 M CH_3OH. The H_2SO_4 and CH_3OH were p.a. grade and the $HClO_4$ was ultra pure. In some experiment p.a. grade $HClO_4$ was also used. The chemicals were purchased from "Merck". All solutions were prepared with high-purity water (Millipore, 18 MΩ cm resistance).

The prepared electrodes were immersed in nitrogen-purged perchloric or sulfuric acid solution to record the basic voltammograms. Methanol was added to the solution while holding the potential at $E = 0.1$ V (RHE). The catalytic activity was measured by recording the potentiodynamic polarization curves with sweep rates of 50 mV s^{-1} and 1 mV s^{-1}.

RESULTS AND DISCUSSION

Model catalysts

Basic voltammograms of Pt(hkl). The basic voltammograms of Pt(*hkl*) in $HClO_4$ solution are given in Fig. 1. Depending on the anodic potential limit, the basic voltammograms show reversible (full line) and ireversible (doted line) processes. The different shapes of the voltammograms clearly suggest the structural sensitivity of both processes. The reversible processes are the adsorption/desorption of hydrogen and hydroxyl anions, hereafter denoted as OH_{ad} species. On the (111) plane, hydrogen adsorption/desorption is determined by a broad wave occurring in the potential region $0.05\text{V} < E < 0.4$ V. This process of the (100) surface occurring at the same potentials as on (111) is defined with a peak at $E_p = 0.35$ V. The hydrogen region is somewhat shorter on the (110) plane, involving the potentials $0.05\text{ V} < E < 0.3$ V in which a sharp peak at $E_p = 0.15$ V appeared. The hydrogen region is followed by OH adsorption/desorption. On the (111) plane, these processes are separated by a so-called double layer region at $0.4\text{ V} < E < 0.6$ V. These two reversible processes are not clearly separated on the other two planes. Adsorption/desorption of OH species takes place at $0.3\text{ V} < E < 0.9$ V on the (110) and at $0.4\text{ V} < E < 0.9$ V on the (111) and (100) planes. It is described by waves on (100), enhancement of currents at (110) and by a "butterfly" peak on (111).

The irreversible process, related to oxide formation, commences at potentials higher than 0.9 V.

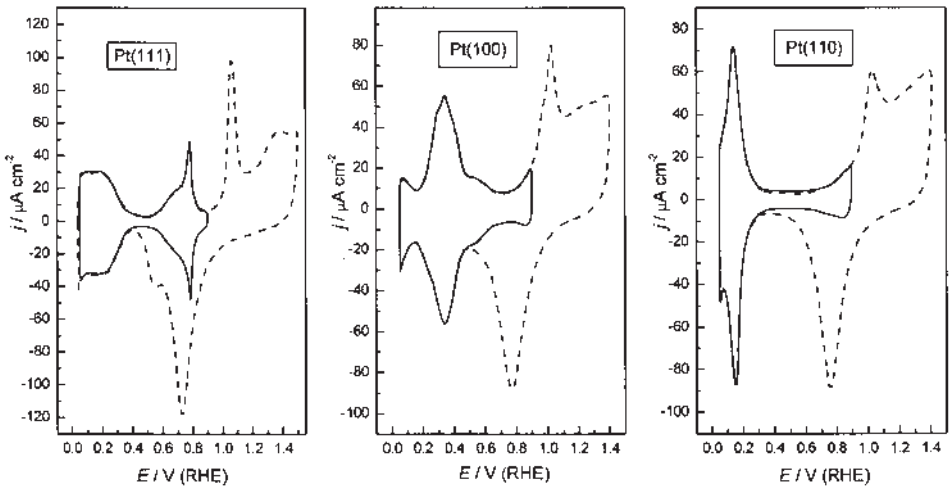

Fig. 1. Cyclic voltammograms for Pt low-index single crystal electrodes up to 0.9 V (full line) and up to 1.4 V (dotted line) in 0.1 M $HClO_4$, v = 50 mV s^{-1}, T = 295 K.

OH_{ad} species participate in methanol oxidation, as is widely agreed, and therefore it is important to determine accurately the initial potentials of its adsorption. In that sense, linear extrapolation of the charging curves showing the dependence of the charge for the adsorption of oxygen containing species on potential (Q *vs.* E) was proposed.[31] The curves Q *vs.* E obtained from the basic voltammograms for Pt(*hkl*) by subtracting the charge for hydrogen desorption from the charge calculation for the anodic part of the voltammogram are presented in Fig. 2. The initial potentials for OH adsorption were estimated by linear extrapolation of the part of Q *vs.* E curve corresponding to OH adsorption to $Q_{OHad} = 0$. On (110) and (100), OH^- anions begin to adsorb at 0.25 V and 0.30 V, respectively, indicating that OH adsorption is coupled to hydrogen desorption. As can be seen from the shape of the Q *vs.* E curve for the (111) plane, the

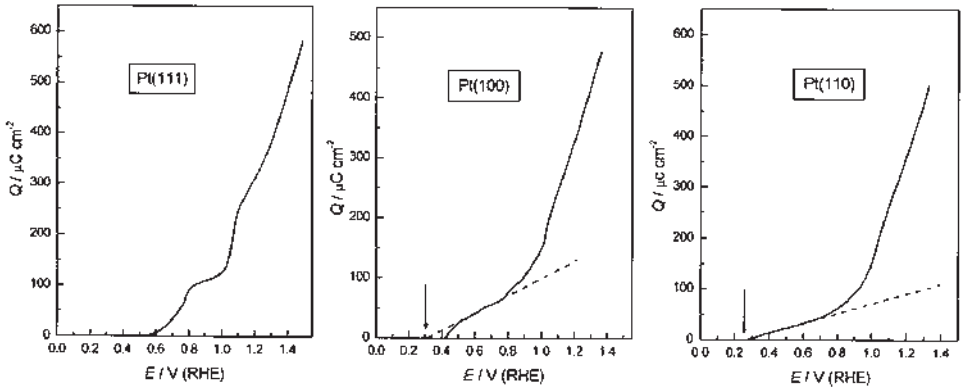

Fig. 2. Dependence of the charge for the adsorption of oxygen containing species on potential for Pt low-index single crystal electrodes in 0.1 M $HClO_4$. Data calculated using the voltammograms in Fig. 1.

linear extrapolation method is not applicable in this case. However, it was proposed that OH adsorbs on (111) in the hydrogen region ($E < 0.4$ V) selectively at defect sites. According to the literature,[31] the change in the slope of the charging curves gives the potential of the reversible/irreversible transition, *i.e.*, the initial potential of oxide formation. At Pt(*hkl*), this potential increases in the sequence (110) < (100) < (111).

Methanol oxidation on Pt(hkl). The voltammograms of methanol oxidation in perchloric acid solution on Pt(*hkl*), recorded in the anodic direction, are given in Fig. 3. The initial potential of the reaction, the potential region in which the reaction takes place and the current are dependent on the single crystal orientation and prove structural sensitivity of the reaction. Methanol oxidation commences firstly on (111), then on (110) and finally on the (100) plane, following the sequences of

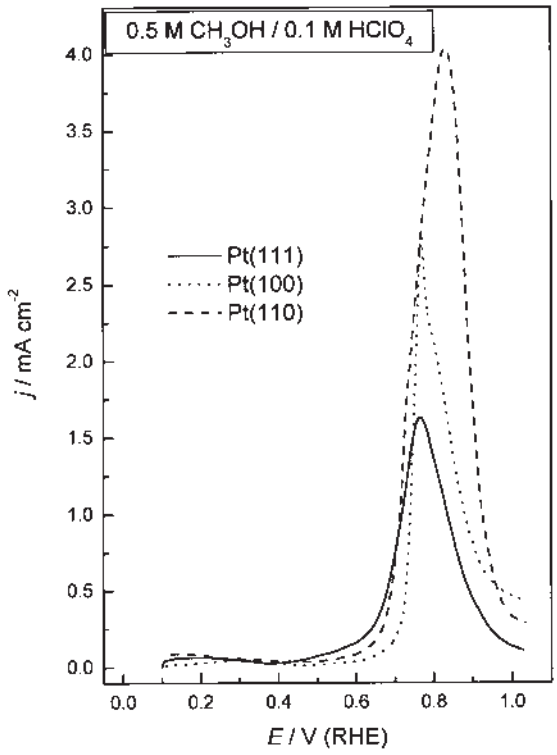

Fig. 3. Voltammograms (first anodic sweeps) for the oxidation of 0.5 M CH_3OH on Pt low-index single crystal electrodes in 0.1 M $HClO_4$, $\nu = 50$ mV s^{-1}; $T = 295$ K.

OH adsorption (Fig. 2). These data support the assumption that the beginning of methanol oxidation is influenced by the beginning of OH adsorption.

Real catalyst

Basic voltammograms of the Pt/C catalyst . The basic voltammograms of the Pt/C catalyst in perchloric and sulfuric acid solutions are shown in Fig. 4. Hydrogen adsorption/desorption, taking place in the potential region between 0.05 V and 0.4 V, is followed by adsorption of oxygen containing species, *i.e.*, first OH_{ad} species at $E < 0.7$ V

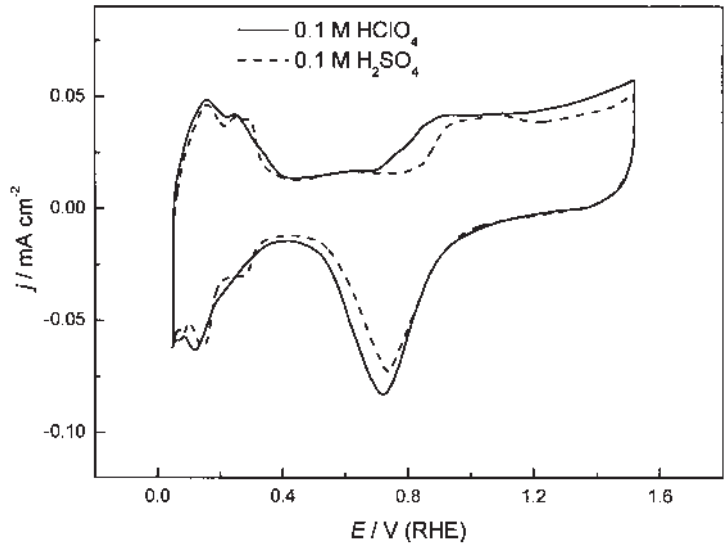

Fig. 4. Cyclic voltammograms for the Pt/C catalyst in 0.1 M $HClO_4$ (full line) and in 0.1 M H_2SO_4 (dotted line). ν = 50 mV s^{-1}; T = 295 K.

and then oxide at higher potentials. The features in the hydrogen region could be rationalized on the basic of hydrogen electrochemistry at Pt(*hkl*) in the same solution (Fig. 1). The H desorption peak at E = 0.15 V can be correlated with (110) sites. The more positive H desorption peak at E = 0.35 V suggests the presence of (100) related facets. The broad and featureless H desorption occurring over the potential range between 0.05 V and 0.4 V below the (110) and (100) peaks indicates the presence of (111) oriented sites. This comparison is consistent with the model of nanoparticles proposed by Kinoshita.[32]

The charging curve for the adsorption of oxygen containing species on the Pt/C catalyst in $HClO_4$ is given in Fig. 5. The intercept at 0.30 V for Q_{OHad} = 0, as well as the change of slope indicates that both OH adsorption and oxide formation are initiated at the same potentials as on the (110) surface in the same solution.

Anions originating from the supporting electrolytes affect the peaks in the hydrogen region, which is in accordance with previously reported data[5] suggesting the presence of absorbed bisulfate anions. However, adsorbed perchlorate anions have not been unequivocally detected. The charge associated with the adsorption/desorption of hydrogen is approximately the same in both acid solutions. Adsorbed bisulfate anions influence the adsorption of OH particles and shift the beginning of oxide formation by ≈ 150 mV towards more positive potentials in the H_2SO_4 compared to the $HClO_4$ electrolyte.

Methanol oxidation on Pt/C. The cyclic voltammogram of methanol oxidation of the Pt/C catalyst in perchloric acid is presented in Fig. 6. Comparison of the data in Figs. 4 and 6 verifies the well-established behavior of methanol oxidation, *i.e.*, the beginning of the reaction (E ≈ 0.4 V) is close to the onset of OH adsorption (E ≈ 0.30 V) and the maximum in the methanol oxidation rate (E ≈ 0.9 V) corresponds to the transition from reversible to irreversible OH adsorption.

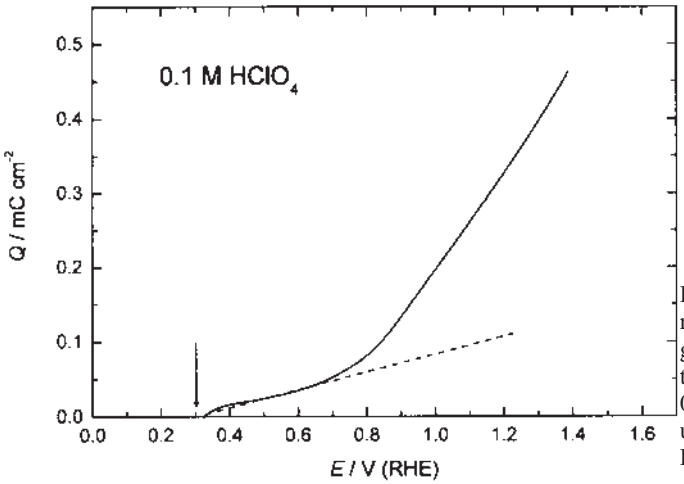

Fig. 5. Dependence of the charge for the adsorption of oxygen containing species on potential for the Pt/C catalyst in 0.1 M $HClO_4$. Data calculated using the voltammogram in Fig. 4.

The effect of anions was examined by contrasting the polarization curves in sulfuric and perchloric acid solutions. Quasi steady-state curves of methanol oxidation recorded at 1 mV s^{-1} are given in Fig. 7. For a comparison, the polarization

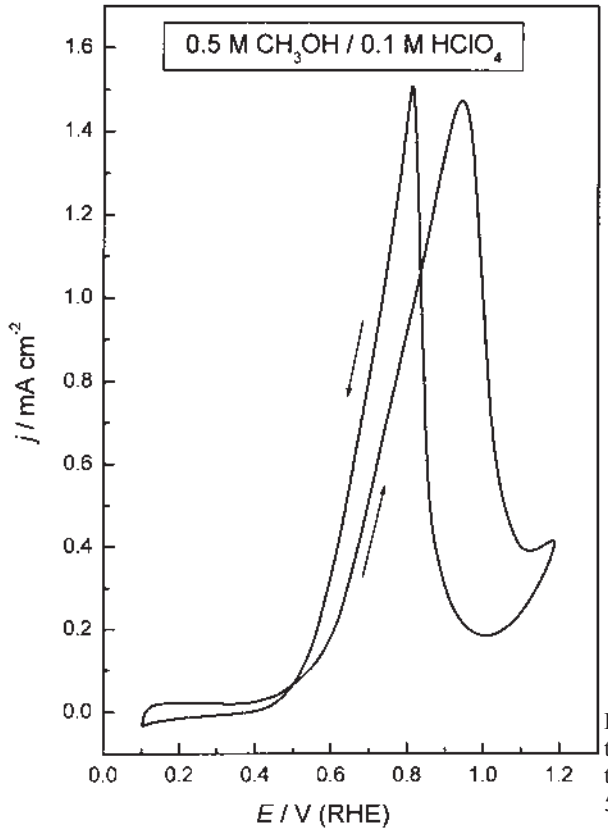

Fig. 6. Cyclic voltammograms for the oxidation of 0.5 M CH_3OH on the Pt/C catalyst in 0.1 M $HClO_4$. ν = 50 mV s^{-1}; T = 295 K.

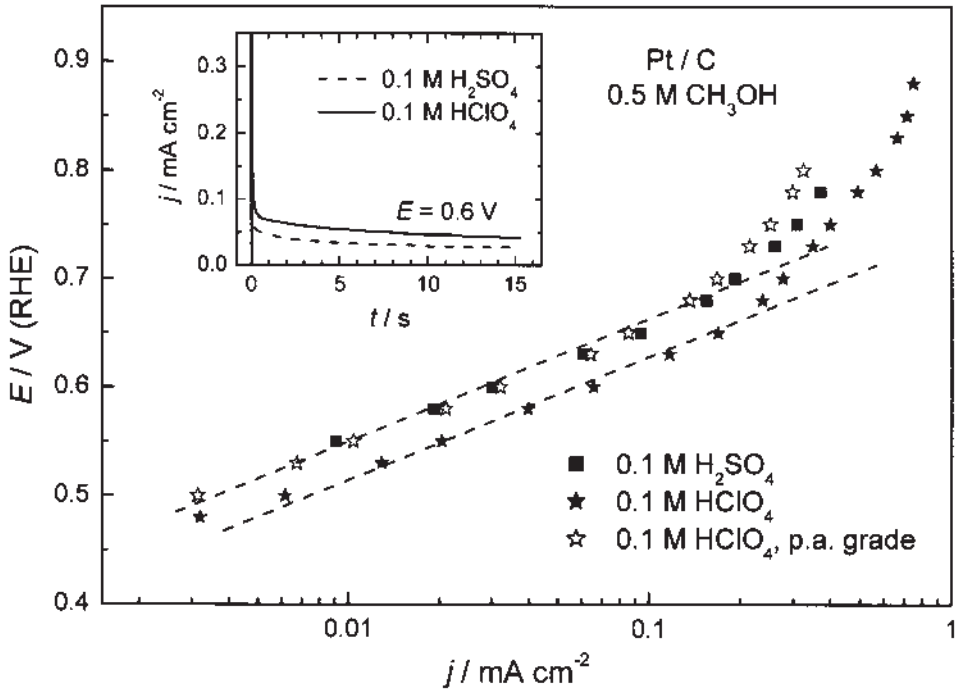

Fig. 7. Tafel plots for the oxidation of 0.5 M CH_3OH on the Pt/C catalyst in different acid solutions. ν = 1 mV s^{-1}; T = 295 K. Inset: Current–time transients of methanol oxidation at E = 0.6 V.

curve in $HClO_4$ (p.a. grade) is also plotted. It can be observed that the methanol oxidation rate is doubled in $HClO_4$ with respect to H_2SO_4. The Tafel slopes are the same, about 120 mV dec^{-1}, indicating that the adsorbed bisulfate anions do not change the reaction path. In order to estimate whether the anions influence the reaction mechanism, more experiments would have to be performed. It is interesting to note that traces of chloride anions in the p.a. grade $HClO_4$ suppress the rate of methanol oxidation to the same extent as 0.1 M bisulfate anions. Such a pronounced effect was not expected because the cyclic voltammograms of Pt/C in both $HClO_4$ solutions almost overlapped. This results stresses the necessity of using high purity $HClO_4$ when the effect on anions is to be examined.

The influence of anions on the methanol oxidation current was confirmed in hronoamperometric measurements. The decay curves presented in the inset in Fig. 7 show that the rate of deactivation of the catalyst at 0.6 V is similar in sulfuric and perchloric acid solution, but the current densities are higher in the perchloric acid solution.

Comparison of methanol oxidation at Pt(hkl) *and Pt/C catalysts*

Figure 8 displeys the quasi steady-state polarization curves for methanol oxidation in $HClO_4$ solution at the model and real catalyst. The activity of the Pt/C catalyst is between the activity of Pt(111) and Pt(110) surfaces. The data for

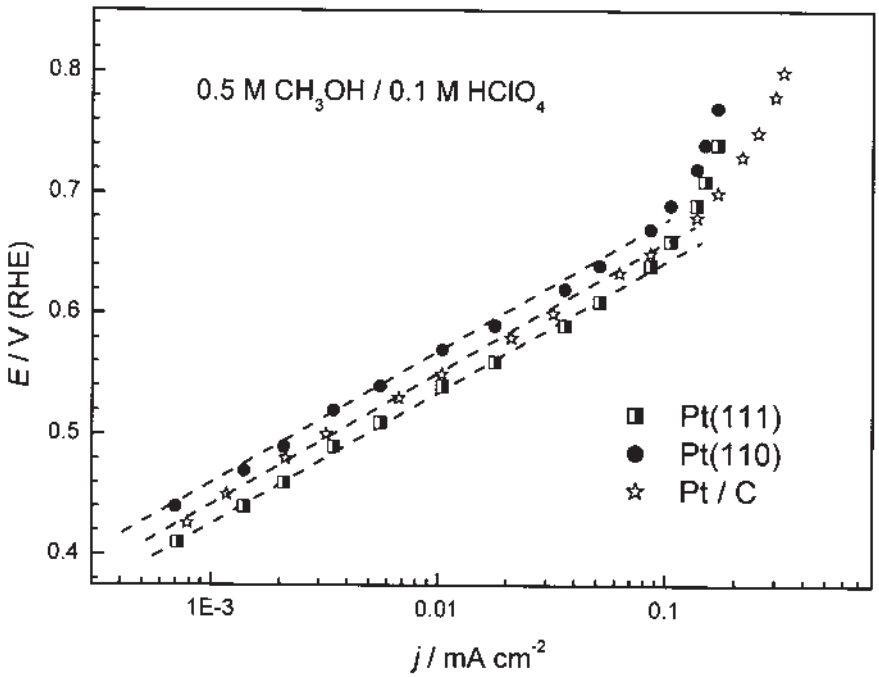

Fig. 8. Tafel plots for the oxidation of 0.5 M CH_3OH on Pt(111), Pt(110) and the Pt/C catalyst in 0.1 M $HClO_4$ solution. $\nu = 2$ mV s^{-1}; $T = 295$ K.

Pt(100) are omitted because of the different mechanism of the reaction, as suggested by the Tafel slope of 60 mV dec^{-1}.

The relationship between the activities of Pt/C, Pt(111) and Pt(110) electrodes agrees with the model of the distribution of crystal planes on the Pt nanoparticles, proposed by Kinoshita.[32] Namely, for Pt particles of ≈ 4 nm (as was found for our catalyst by XRD, TEM, STM and cyclic voltammetry), surface (111) and rough (110) regions dominate, in the ratio of 65 % and 22 %, respectively. Plane (100) amounts to 13 % of the total surface of the particles and its ratio increases with increasing particle size.

TABLE II. Correlation between the initial potentials of OH adsorption and methanol oxidation on Pt single crystals and the supported nanocatalyst

	PT (111)	Pt(110)	Pt / C
$E_{initial}$ OH_{ad}	< 0.40 V	≈ 0.25 V	≈ 0.30 V
$E_{initial}$ CH_3OH_{ox}	≈ 0.40V	≈ 0.45 V	≈ 0.40 V

The similarity of the kinetics of methanol oxidation on Pt/C and single crystal planes Pt(111) and Pt(110) suggests that the reaction mechanism is probably the same. According to Iwasita,[1] on Pt(111) and Pt(110) in the potential region from 0.4 V to 0.7 V, the rate determining step is oxidation of the adsorbed residues of

methanol. Gasteiger *et al.*[33] assumed that oxidative removal of CO_{ad} in a Langmuir–Hinshelwood type of reaction:

$$CO_{ad} + OH_{ad} \rightarrow CO_2 + H^+ + e^- \quad (2)$$

is the rate determining process. The connection between the onset of methanol oxidation and the adsorption of OH species, presented in Table II, follows this conclusion. At higher potentials, the slope of the Tafel plot increases. This change is provoked by the formation of irreversibly adsorbed oxide, rendering the Pt surface less active for methanol adsorption.

CONCLUSIONS

On the basic of the investigation of the methanol oxidation on Pt single crystals and high surface area carbon supported Pt particles, the following can be concluded:

* A correlation between the beginning of adsorption of OH_{ad} species and methanol oxidation has been established based on the linear extrapolation method and on cyclic voltammograms in a supporting electrolyte for Pt(*hkl*) (model catalyst) and Pt/C catalyst (real catalyst).

* The electrocatalytic activity of the catalysts for methanol oxidation increases in the sequence Pt(110) < Pt/C < Pt(111), suggesting that the activity of the supported Pt catalyst can be correlated with the activities of the sites dominating in the Pt particles. This sequence is in accordance with the Kinoshita model of the surface distribution of the crystal faces of a Pt nanoparticle.

* It was shown that anions (bisulfates or chlorides) originating from the supporting electrolyte suppress rate of the methanol oxidation but do not influence the reaction path.

Acknowledgement: This work was financially supported by the Ministry of Science and Environmental Protection of the Republic of Serbia, Contract No. H-142056.

ИЗВОД

ОКСИДАЦИЈА МЕТАНОЛА НА ПЛАТИНСКИМ ЕЛЕКТРОДАМА У КИСЕЛОЈ СРЕДИНИ: ПОРЕЂЕЊЕ МОДЕЛ И РЕАЛНИХ КАТАЛИЗАТОРА

А. В. ТРИПКОВИЋ[а], С. Љ. ГОЈКОВИЋ[б], К. Ђ. ПОПОВИЋ[а] и Ј. Д. ЛОВИЋ[а]

[а]*ИХТМ-Центар за електрохемију, Универзитет у Београду, Његошева 12, П. П. 473, 11000 Београд и* [б]*Технолошко-металуршки факултет, Универзитет у Београду, Карнегијева 4, П. П. 3503, 11000 Београд*

Оксидација метанола испитивана је на нискоиндексним Pt монокристалним електродама (модел катализатор) и на нанокатализатору Pt диспергованом на активном угљу као носачу (реални катализатор) у киселој средини. Метода линеарне екстраполације кривих зависности количине наелектрисања адсорпције кисеоничних честица од потенцијала коришћена је за одређивање почетка адсорпције ОН анјона. Потврђено је да је адсорпција ОН честица структурно осетљива реакција и показана је корелација са почетком реакције оксидације метанола. Утврђено је да бисулфатни и хлоридни анјони из носећег електролита смањују брзину оксидације метанола, али вероватно не утичу на реакциони пут. Електрокаталитичка активност испитиваних катализатора

расла је у низу Pt(110) < Pt/C < Pt(111) указујући на то да се активност Pt нанокатализатора може повезати са уделима нискоиндексних равни на површини Pt наночестице.

(Примљено 8. децембра 2005, ревидирано 15. марта 2006)

REFERENCES

1. T. Iwasita, in *Handbook of Fuel Cells – Fundamentals, Technology and Apoplications,* Ed. W. Viestich, H. A. Gasteiger, A. Lamm), Vol. 2, Wiley, New York
2. L. Carett, K. A. Friedrich, U. Stimming, *Fuel Cells.* **1** (2001) 5
3. R. Parsons, T. Vander Noot, *J. Electroanal. Chem.* **257** (1988) 9
4. B. Beden, J. M. Leger, C. Lamy, in: *Modern Aspects of Electrochemistry*, Vol. 22, Eds. J. O'M. Bockris, B. E. Conway, R. E. White, Plenum press, New York, 1992
5. N. M. Markovic, P. N. Ross, Jr., *Surface Sci. Reports* **45** (2002) 117
6. T. D. Jarvi, E. M. Suve in: *Electrocatalysis*, Eds. J. Lipkovski, P. N. Ross, Wiley, New York, 1998
7. A. Hamnett, in: *Intefacial Electrochemistry*, Ch. 47, Ed. A. Wieckowski, Marcel Dekker, New York, 1999
8. E. Herrero, K. Franasczczuk, A. Wieckowski, *J. Phys. Chem.* **98** (1994) 5074
9. V. S. Gatotyzky, Yu. B. Vassiliev, *Electrochim. Acta* **12** (1967) 1323
10. O. A. Petrii, B. I. Podlovchenko, A. N. Frumkin, H. Lal, *J. Electroanal. Chem.* **10** (1965) 253
11. R. R. Adžić, A. V. Tripković, W. O'Grady, *Nature* **296** (1982) 137
12. J. Clavilier, C. Lamy, J. M. Leger, *J. Electroanal. Chem.* **125** (1981) 249
13. V. S. Bagotzki, Yu. B. Vassiliev, O. A. Kazova, *J. Electroanal. Chem.* **81** (1977) 229
14. S. Juanto, B. Beden, F. Hahn, J. M. Leger, C. Lamy, *J. Electroanal. Chem.* **237** (1987) 119
15. S. C. Chang, L. W. H. Leung, M. J. Weaver, *J. Phys. Chem.* **94** (1990) 6013
16. X. H. Xia, T. Iwashita, F. Ge, W. Vielstich, *Electrochim. Acta* **41** (1996) 711
17. S. Gilman, *J. Phys. Chem.* **68** (1964) 70
18. P. A. Christensen, A. Hamnett, G. L. Troughton, *J. Electroanal. Chem.* **362** (1993) 207
19. N. M. Markovic, T. J. Schmidt, B. N. Grgur, H. A. Gasteiger, P. N. Ross, Jr., R. J. Behm, *J. Phys. Chem. B* **103** (1999) 856
20. H. Kim, I. Rabelo de Moraes, G. Tremilosi-Filho, L. Haasch, A. Wieckowski, *Surf. Sci.* **474** (2001) 1203
21. A. V. Tripković, K. Dj. Popović, J. D. Lović, V. M. Jovanović, A. Kowal, *J. Electroanal. Chem.* **572** (2004) 119
22. S. Park, Y. Xie, M. J. Weaver, *Langmuir* **18** (2002) 679
23. A. V. Tripković, K. Dj. Popović, B. N. Grgur, B. Blizanac, P. N. Ross, N. M. Marković, *Electrochim. Acta* **47** (2002) 3707
24. J. Jiang, A. Kucernak, *J. Electroanal. Chem.* **576** (2005) 223
25. J. Clavilier, R. Faure, R. Guinet, R. Durand, *J. Electroanal. Chem.* **107** (1980) 205
26. T. J. Schmidt, M. Noeske, H. A. Gasteiger, R. J. Behm, P. Britz, W. Brijoux, H. Bonnemann, *Langmuir* **13** (1997) 2591
27. J. D. Lović, S. Lj. Gojković, K. Dj. Popović, D. V. Tripković, A. V. Tripković, *Mat. Sci. Forum* (2005) in press
28. A. V. Tripković, K. Dj. Popović, J. D. Lović, *J. Serb. Chem. Soc.* **68** (2003) 849
29. J. D. Lović, A. V. Tripković, S. LJ. Gojković, K. D. Popović, D. V. Tripković, P. Olszewski, A. Kowal, *J. Electroanal. Chem.* **581** (2005) 294
30. F. Gloaguen, J. M. Leger, C. Lamy, A. Marmann, U. Stimming, R. Vogel, *Electrochim. Acta* **44** (1999) 1805
31. . J. Schmidt, P. N. Ross, Jr., N. M. Marković, *J. Phys. Chem. B* **105** (2001) 12082
32. K. Kinoshita, *J. Electrochem. Soc.* **137** (1990) 845
33. H. A. Gasteiger, N. Markovic, P. N. Ross, E. J. Cairns, *J. Phys. Chem. B* **97** (1993) 12020.